# Star formation and ionized regions in the Inner Galactic Plane.

**P. Palmeirim**[1]**, A. Zavagno**[2]**, and D. Elia**[3]

[1] Instituto de Astrofísica e Ciências do Espaço, Universidade do Porto, CAUP, Rua das Estrelas, PT4150-762 Porto, Portugal
[2] Aix Marseille Univ, CNRS, LAM, Laboratoire d'Astrophysique de Marseille, Marseille, France
[3] Istituto di Astrofisica e Planetologia Spaziali INAF-IAPS, via Fosso del Cavaliere 100, I-00133 Roma, Italy

## Abstract

We present a comprehensive statistical study to understand the impact of galactic bubble structures detected in the *Spitzer* observations throughout the galactic plane on the star formation process. We analysed 1 360 galactic bubbles and ∼70 000 star-forming sources, from both Hi-GAL and GLIMPSE surveys, located in their vicinity. The spatial distribution of the star-forming sources seen in surface density maps reveal a clear evolutionary gradient, were more evolved Young Stellar Objects (YSOs) are typically found in the center, while recent star-forming sources (prestellar and protostellar) can be seen at the edges of the bubbles.

Based on the dynamic ages derived for the bubbles and numerical simulations we find that the timescale for star-formation are better describe advocating for the pre-existence of density structures in the medium prior to the creation of the ionizing source(s).

Identical pattern of age distribution of star-forming sources has been found in a recent detailed study of the nearby $\lambda$ Ori bubble using APOGEE-2 and GAIA DR2 observations, which provides compelling evidence of what we obtained in our statistical result. In light of these results we propose a scenario for the star formation process in expanding ionizing bubbles.

## 1 Introduction

*Spitzer* images at 8 $\mu$m and 24 $\mu$m reveal an almost ubiquitous presence of bubble structures throughout the entire Galactic Plane [4, 5]. These bubbles are associated to H II regions that are generated by massive stars that ionize the surrounding medium, causing it to expand isotropically. The expansion against the surrounding cold molecular medium may induce the triggering of star formation as shown in several observational studies [28, 29, 7, 21, 15].

This study aims to understand the relation between the presence of an H II region, its expansion and how star formation is progressing in its vicinity by combining information of Galactic Plane surveys in a large sample of Galactic bubbles.

## 2    Statistical Sample

We made use of the The Milky Way Project (MWP) catalog [22] of bubbles extracted from Spitzer-GLIMPSE 8 $\mu$m and 24 $\mu$m maps and selected 1 360 bubbles with radii larger than $72''$ to ensure that the bubbles were resolved in the *Herschel* maps. We searched for all star-forming sources that were found within four times the effective radius of a bubble.

The YSO candidates were selected from the GLIMPSE catalog by following the same approach as [10]. Subsequently, they were further classified into different evolutionary stages Class I and Class II according to both their infrared spectral index [13] and their position in the IRAC color-color diagram [2]. This led to a total sample of 10 694 Class I and 18 209 Class II sources. Class III YSOs were excluded due to the high level of contamination of asymptotic giant branch (AGB) stars in the Galactic Plane that harbour thin disks that can mimic the SED of class III YSOs [19].

To probe the most recent star formation activity we made use of the Hi-GAL source catalog [8] and found a total sample of 25 911 prestellar (gravitationally bound) and 14 918 protostellar (based on 70 $\mu$m detection) clumps at the vicinity of our sample of bubbles.

This lead to a final sample of $\sim$70 000 star-forming sources at different evolutionary stages located towards 1360 bubbles.

## 3    Results

### 3.1    Spatial distribution and evolutionary gradient of star-forming sources

The spatial information of all the star-forming sources located towards the 1 360 galactic bubbles was compiled into surface density maps (see Fig. 1). These maps are spatially normalized by the bubble radius and display the location of all star-forming source at a given evolutionary stage. The surface density maps reveal how star-forming sources follow a clear evolutionary trend, where more evolved star-forming objects are found spatially located near the center, while younger star-forming objects are found at the edge of the bubbles. Furthermore, considering all the star-forming sources we find $\sim$80% more star-forming objects per unit area toward the direction of bubbles compared with their surrounding outer fields.

### 3.2    Dynamic age estimates of the bubbles

Considering that the 1 360 bubbles are at different stages of their expansion we derived dynamic ages for a subsample of 182 HII regions, for which kinematic distances and radio continuum flux measurements were available, by following the approach presented in Tremblin et al. (2014)[23]. The analytical solutions and numerical simulations performed in their paper
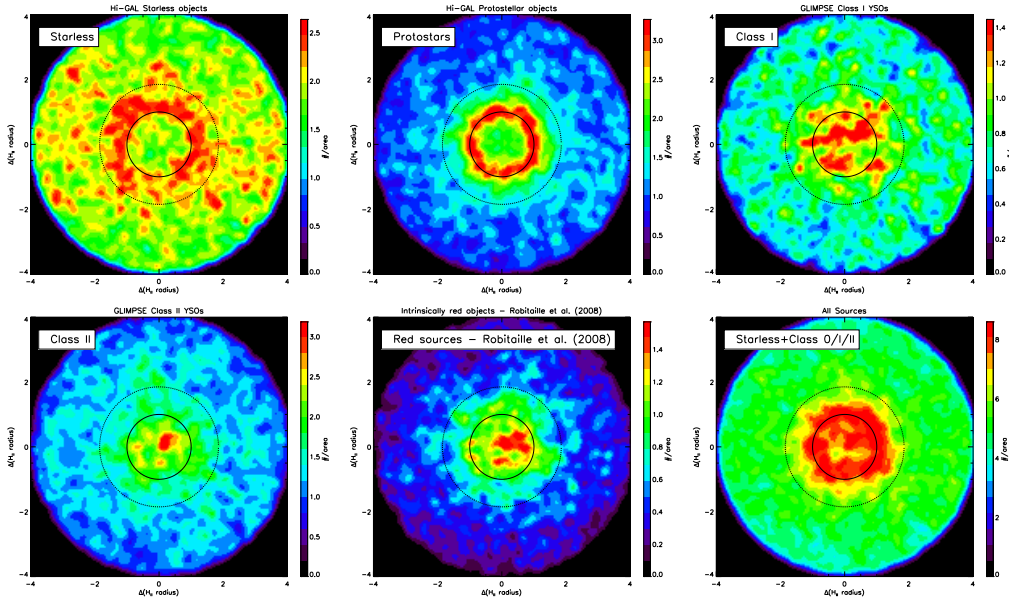
Figure 1:   Surface density maps for all star-forming objects - Hi-GAL clumps, IRAC YSOs and intrinsically red sources from [19] - associated to the bubble sample. The spatial scale of the maps are normalized by the bubble radius (solid black circle). The dash black circle represents the average shell radius.

demonstrated that the expansion of H II regions is slowed down by turbulent ram pressure ($P_{turb}$) of the environment until it reaches quasi-static equilibrium with the pressure of the ionized gas ($P_{II}$). With the use of radio continuum flux measurements and by applying the Larson laws (see [14]) to infer $P_{II}$ and $P_{turb}$, respectively, dynamic age estimates were obtained by comparing the results with the isochrones provided by the grid of 1D models of expanding H II regions. The derived dynamic ages are in good agreement with the photometric ages of the ionizing stars in well-known regions (e.g., Rosette, RCW 36, RCW 79, and M16)[23].

Following this approach we derived dynamic ages for the 182 bubbles with distance determination (obtain from the WISE catalog of Galactic H II regions [3]) and radio continuum flux measurements (1.4 GHz and 4.85 GHz from the NVSS [6] and PMNS [27], respectively). In Fig. 2a) we present a top view of the location of the 182 bubbles in the Galactic plane, with their respective dynamic ages and sizes. We find that the majority of the of the bubbles follow the Galactic spiral arms and have ages younger than 4 Myr (~80%), which can be related with the typical lifetime of high-mass stars (a main-sequence spectral type O5 star, for example, has an expected lifetime of ~4 Myr [1].

### 3.3   Clump formation efficiency

To better comprehend the impact of H II regions on the star formation process we need to understand how efficient the conversion of cold neutral matter collected in their shells com-
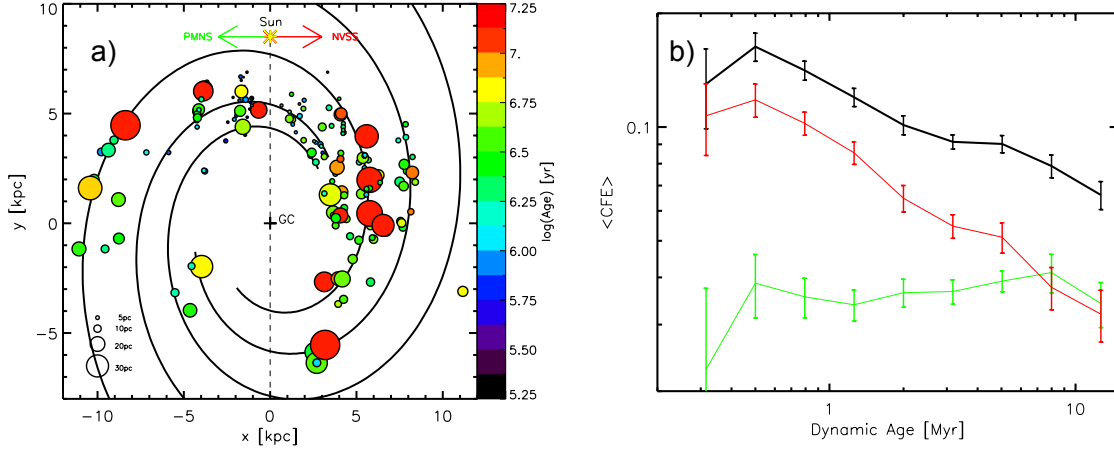
Figure 2: **a)** Bubble distribution in Galactocentric coordinates with their respective diameter and age. The black solid curves represent the position of the 4 Galactic spiral arms based on [20]. **b)** CFE of the Hi-GAL star-forming clumps as a function of the dynamic age of the bubbles (solid black), prestellar (solid green), and protostellar (solid red) sources.

pares with region that are not affected by feedback processes. The clump formation efficiency (CFE) was determined by calculating the ratio between the masses of the bubbles and the masses of the respective associated Hi-GAL sources (prestellar and protostellar clumps). We obtained a CFE ∼15% for the Hi-GAL star-forming sources, which means that typically ∼15% of the molecular gas around the bubbles are concentrated in the form of prestellar or protostellar clumps. This value is a factor of ∼2 higher than the CFE estimated outside the bubbles and compared with other well-known active star-forming regions (e.g., RCW106[17] and W43[16]).

In Fig. 2b) we can see how the CFE varies with the evolution of the bubbles. Interestingly, we find that CFE for protostellar clumps tends to decrease with the age of the bubble, while CFE of prestellar clumps seems to remain nearly constant. We interpret this trend as a possible increase in the formation rate from the prestellar to protostellar phase at the early stages of the bubble expansion, which would eventually decrease as the impact of the expansion and the ionization weakens.

## 4    Conclusions

The evolutionary gradient seen in the spatial distribution of star-forming sources sets strong constrains in the star formation mechanisms around ionizing sources. A large number of the Class II YSOs are found in the inner parts of bubbles that have younger dynamic ages than the typical lifetime of low- and intermediate-mass Class II objects $\sim 2 \pm 1$ Myr [9]. This suggests that these YSOs have probably undergone their formation process prior to the expansion of the bubble, possibly as part of the same star-forming complex that gave birth

to the ionizing massive stars that are responsible for the expansion of the bubbles. This is consistent with the fact that in cluster-forming environments, massive stars are expected to form after low-mass stars have completed their accretion phase [12]. Furthermore, the shell fragmentation times estimated (following [26]) to understand if gravitational instability of the shells alone could be responsible for the triggering showed that a significant fraction of bubble shells would in fact not have had time to fragment. Thus, we advocate that dense structures existed in the medium prior to the bubble expansion to allow for a more comparable star-formation timescale, as shown in the simulations performed in [24, 25]. Furthermore, the fraction of clumps that is spatially associated with bubbles is ∼23%, consistent with the fraction of ATLASGAL clumps in the vicinity of MWP bubbles (Kendrew et al. 2016). However, for the individual fraction of protostellar clumps we obtain 41%. Thus, we argue that the higher fraction of protostellar clumps may be related with the higher protostellar clump formation rate in bubbles, as discussed in Sect. 3.3.

A recent study [11] combining APOGEE-2 and GAIA observations of the $\lambda$ Ori bubble located in the nearby Orion molecular cloud complex revealed, with a very high detail, how older YSOs are clustered in the center of the bubble while younger at scattered around the center. In particular, the YSOs are moving radially away from the center with the further away sources moving faster. This result is in completely consistent with what we found in our statistical analysis and interpretation of our galactic bubbles sample, which could indeed describe a more universal process of formation and evolution of star formation in ionizing bubbles.

Based on the results from Palmeirim et al. (2017)[18] here summarized, we propose a scenario for the process of star formation in ionizing expanding bubbles. 1) Formation of low- and intermediate-mass stars is undergoing prior to the formation of the massive ionizing star(s); 2) As the medium is expanding due to the ionizing pressure more evolved star-forming sources which are denser are less influenced than the more diffused cold neutral matter; 3) the cold molecular matter is accumulate in the shell of the bubbles and fragments into stars via gravitational instabilities as the bubble expands.

## Acknowledgments

## References

[1] Allen, C. W. 1973, Astrophysical quantities

[2] Allen, L. E., Calvet, N., D'Alessio, P., et al. 2004, ApJS, 154, 363

[3] Anderson, L. D., Bania, T. M., Balser, D. S., et al. 2014, VizieR Online Data Catalog, 221

[4] Churchwell, E., Povich, M. S., Allen, D., et al. 2006, ApJ, 649, 759

[5] Churchwell, E., Watson, D. F., Povich, M. S., et al. 2007, ApJ, 670, 428

[6] Condon, J. J., Cotton, W. D., Greisen, E. W., et al. 1998, AJ, 115, 1693

[7] Deharveng, L., Schuller, F., Anderson, L. D., et al. 2010, A&A, 523, A6

[8] Elia, D., Molinari, S., Schisano, E., et al., 2017, MNRAS, 471, 100

[9] Evans, II, N. J., Dunham, M. M., Jørgensen, J. K., et al. 2009, ApJS, 181, 321

[10] Gutermuth, R. A., Megeath, S. T., Myers, P. C., et al. 2009, ApJS, 184, 18

[11] Kounkel, M., Covey, K., Suárez, G., et al. 2018, AJ, 156, 84

[12] Kumar, M. S. N., Keto, E., & Clerkin, E. 2006, A&A, 449, 1033

[13] Lada, C. J., Muench, A. A., Luhman, K. L., et al. 2006, AJ, 131, 1574

[14] Larson, R. B. 1981, MNRAS, 194, 809

[15] Liu, H.-L., Li, J.-Z., Wu, Y., et al. 2016, ApJ, 818, 95

[16] Nguyen Luong, Q., Motte, F., Schuller, F., et al. 2011, A&A, 529, A41

[17] Nguyen, H., Nguyen-Luong, Q., Martin, P. G., et al. 2015, ApJ, 812, 7

[18] Palmeirim, P., Zavagno, A., Elia, D. et al. 2017, A&A, 605, A35

[19] Robitaille, T. P., Meade, M. R., Babler, B. L., et al. 2008, AJ, 136, 2413

[20] Russeil, D. 2003, A&A, 397, 133

[21] Samal, M. R., Zavagno, A., Deharveng, L., et al. 2014, A&A, 566, A122

[22] Simpson, R. J., Povich, M. S., Kendrew, S., et al. 2012, MNRAS, 424, 2442

[23] Tremblin, P., Anderson, L. D., Didelon, P., et al. 2014, A&A, 568, A4

[24] Walch, S., Whitworth, A. P., & Girichidis, P. 2012, MNRAS, 419, 760

[25] Walch, S., Whitworth, A. P., Bisbas, T. G., Hubber, D. A., & Wünsch, R. 2015, MNRAS, 452, 2794

[26] Whitworth, A. P., Bhattal, A. S., Chapman, S. J., Disney, M. J., & Turner, J. A. 1994, MNRAS, 268, 291

[27] Wright, A. E., Griffith, M. R., Burke, B. F., & Ekers, R. D. 1994, ApJS, 91, 111

[28] Zavagno, A., Pomarès, M., Deharveng, L., et al. 2007, A&A, 472, 835

[29] Zavagno, A., Russeil, D., Motte, F., et al. 2010, A&A, 518, L81